

Spin-dependent magnetoresistance and spin-charge separation in multiwall carbon nanotubes

X. Hoffer, Ch. Klinke, J.-M. Bonard, L. Gravier
 IPN, Faculté des Sciences de Base, EPFL, 1015 Lausanne, Switzerland.

J.- E. Wegrowe*
 Laboratoire des Solides Irradiés, Ecole polytechnique, 91128 Palaiseau Cedex, France.

(Dated: November 5, 2021)

The spin-dependent transport in multiwall carbon nanotubes obtained by chemical vapor deposition (CVD) in porous alumina membranes is studied. The zero bias anomaly is found to verify the predicted Luttinger liquid power law. The magnetoresistance at high fields varies in sign and amplitude from one sample to the other, which is probably due to the presence of dopant in the tube. In contrast, the magnetoresistance due to the spin polarized current is destroyed in the nanotube as expected in case of spin-charge separation.

PACS numbers: 73.63.Fg (Electronic transport in nanotubes), 72.15.Nj (Collective modes), 72.25.Hg (Electrical injection of spin polarized carriers)

Carbon multiwall nanotubes (MWNT) and single wall nanotubes (SWNT) are considered as one of the most promising building blocks for nanoelectronics and molecular electronics. Among the large variety of possible applications, a development in the framework of spintronics [1] is naturally invoked, leading to studies of spin-dependent transport in carbon nanotubes [2, 3, 4, 5]. In this context, the spin dependent magnetoresistance (SD-MR) of a MWNT contacted between two ferromagnetic electrodes has been measured as a function of the magnetization direction of the ferromagnetic contacts. Beyond the interest in spintronics applications, the study of such magnetic systems allows the investigation of fundamental questions about the role of the spin degrees of freedom in quantum wires or Luttinger liquids (LL) [6, 7], where a specific behavior is expected due to spin-charge separation [8, 9, 10, 11].

In the present work we observed LL-like behavior in samples consisting of one or a few nanotubes connected to a tunneling junction. We use the typical scaling law $G \propto V_{bias}^\alpha$ at high voltage bias V_{bias} , and $G \propto T^\alpha$ at low voltage bias (G is the conductance, T the temperature and α is the scaling coefficient), as discussed recently in the literature for SWNT and MWNT [12, 13, 14, 15, 16]. This scaling law originates in the framework of the Luttinger liquid (LL) theory [8, 17, 18] in 1D quantum wires, or intrinsic Coulomb blockade in MWNT [19], or in the framework of the environmental Coulomb Blockade (ECB) theory applied to quantum wires [20, 21]. The spin-dependent magnetoresistance, related to the magnetic hysteresis of the contacts, is measured for each sample and related to the scaling coefficient α in order to observe an effect of the expected spin-charge separation. Our measurements confirm previous (negative) observations revealing that the SD-MR is very small [4, 5] for

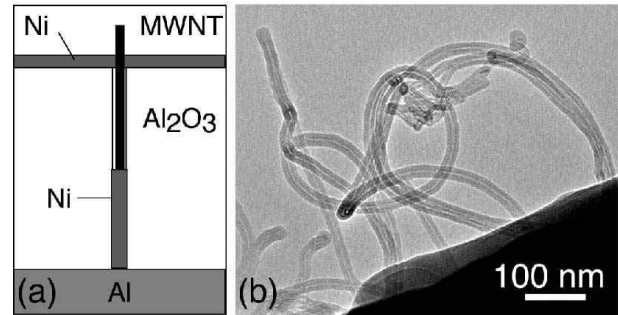


FIG. 1: (a) Schematics of the Ni/MWNT heterostructure. (b) TEM micrograph of NTs emerging from the pores at the membrane surface.

all measured tubes; a significant signal is measured only at vanishing bias [3] or for small tubes where the role of the junctions becomes significant. These measurements indicate that the nanotubes destroy the spin polarization of the current.

The MWNT were grown by a CVD technique in nanoporous alumina membranes (see Fig. 1a)). The membranes are obtained by anodization of Al [5], and the length of the pores in the membrane is $1.5 \mu\text{m}$. Ni wires of controlled length are then electrodeposited in the pores [23]. The diameter of the MWNT are fixed at $23 \text{ nm} \pm 2$ as shown by TEM (Fig. 1b). The membrane is then exposed to 20 mbar acetylene under 650°C in a tube furnace during 5 min in order to activate the catalytic growth of MWNTs from the top of the electrodeposited Ni wires. After nanotube deposition (see Fig. 1b), the tubes are kept in air for a few minutes before a Ni layer (100 nm thickness) is deposited with sputtering on top of the membrane. The exposure to air leads to the formation of a thin C-oxide layer which plays the role of a tunneling junction at low temperature. This tunneling junction is exploited for tunneling spectroscopy. We have studied a statistical ensemble (40) of samples. Each

*Electronic address: wegrowe@hplsesi.polytechnique.fr

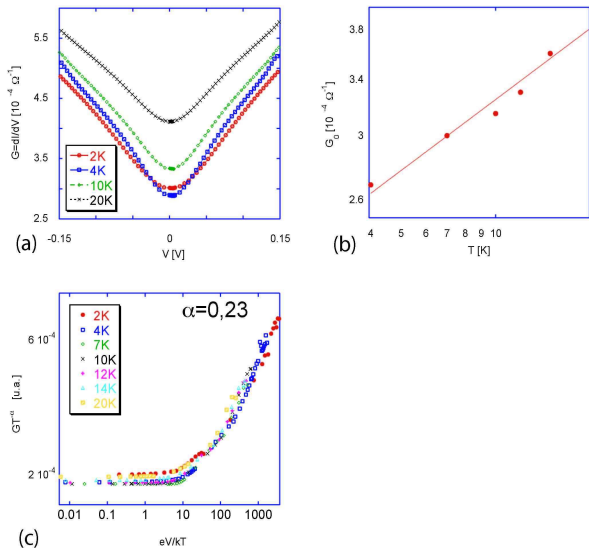


FIG. 2: Sample A. (a) Conductance G ($10^{-4} \Omega^{-1}$) as a function of eV_{bias} for various temperatures. (b) Log-Log plot of the temperature dependence of the zero bias conductance as a function of the temperature. The line is a power law with $\alpha=0.23$. (c) Scaling $GT^{-\alpha}$ as a function of the ratio (eV_{bias}/kT).

sample is defined by two sets of parameters, namely the intrinsic parameters (length, purity of the tube, presence of kinks) and the environmental conditions. The latter are described in terms of circuit theory by the impedance of tunneling junctions, influence of other tubes contacted in parallel, and other sources of dissipation. The magnetic characteristics of the ferromagnetic contacts also vary from one sample to the other, but the magnetic configurations in such structures are well known from anisotropic magnetoresistance (AMR) [23] and domain wall scattering (DWS) [23] measurements.

The resistances range within $1k\Omega$ to $100 k\Omega$ for the 40 samples measured. The contribution of both the tunneling junction and the Ni wire to the resistance can be estimated from the $R(T)$ profiles. The scaling law is presented in Fig. 2 for a typical MWNT of length of about 600 nm (sample **A**, the resistance at $2K$ is $5 k\Omega$). The differential conductance $G = dI/dV$ is first plotted as a function of the bias voltage V_{bias} for different temperatures in Fig. 2(a), showing a typical zero bias anomaly (ZBA). The values at zero bias $G(V_{bias}=0)$ follow the power law T^α with $\alpha = 0.23$ (Fig. 2(b)). In Fig. 2(c), $GT^{-\alpha}$ is plotted as a function of eV_{bias}/kT . All data collapse on a unique curve, which indicates a LL-like behaviour.

Within the ensemble of 40 samples, 25 follow the scaling law for the ZBA, which defines the coefficient α which

are shown in Fig 3 (e.g. sample **A,C** and **D**). Five samples show no significant ZBA (Ohmic behavior : $\alpha=0$), and about 10 show a strong ZBA, but without scaling law (e.g. sample **B**). The coefficient α is distributed within the interval $0 \leq \alpha \leq 1$ (Fig. 3). In the framework of the transmission line approach we have $\alpha = 2Re(Z)/R_0$, where $R_0 = h/e^2$ is the quantum resistance and Z is the impedance of the transmission line (e.g. $Z = R \approx \sqrt{L/C}$ with the impedance L and the electrostatic capacitance C). The theoretical value for a LL without taking into account the environment is $\alpha_0 \approx 0.24$ [8, 17, 18, 20]. In a first approximation, the coefficient α is expected to be below the ideal value α_0 if the number of transmission modes N is enhanced (typically $\alpha \propto \sqrt{1/N}$ [20]), e.g. due to the large number of walls or impurities. On the other hand, α should be larger than the bulk value if structural defects, like kinks, are present [14].

The correlation between α and the length l of the tube is plotted in Fig. 3. The length is estimated from the deposition time of the Ni. Taking into account that the probability of the presence of a kink or defect in the tube is proportional to the length of the tube, we expect to measure scaling coefficients $\alpha \leq \alpha_0^*$ for small l only, and $\alpha \geq \alpha_0^*$ for large l . This is indeed observed in Fig. 3, where there is no sample verifying $\alpha \geq \alpha_0^*$ below $l=500\text{nm}$ (TEM measurements confirm that there is a vanishing probability to find a kink at this scale), and no sample verifying $\alpha \leq \alpha_0^*$ above $l=900 \text{ nm}$. The general tendency depicted in Fig. 3 is then interpreted as the presence of kinks or defects in long CVD grown nanotubes. The large numbers of very small values of coefficient α for small tubes (below 300 nm) can be interpreted as an effect of screening of the tube by the contacts.

If the transport properties at zero magnetic field can be described with a single parameter α , the MR properties are far more versatile and various kinds of signals have been reported in the literature [2, 3, 4, 5]. We separate below two different types of MR, the direct MR due to the direct action of the magnetic field on the charge, and the spin-dependent magnetoresistance due to the spin polarized current. The MR has been measured for each sample with a field perpendicular to the tube axis between $\pm 5T$. At fields above $1.5 T$, the magnetization is saturated, and the profile gives the direct MR of the nanotube. As already reported in the literature, the observed MRs (Fig. 4) are either positive (the resistance increases with increasing magnetic field) or negative, varying from one sample to the other. Except for the sign, both positive and negative MR are rather similar, with in some cases a transition from positive to negative MR at low temperature (Fig. 4(a)). Statistically, magnetoresistance at $2.5K$ is positive in 50 % of the samples and negative in 25 %, while 25 % have no measurable trend (no MR at high field). We do not observe any correlation of the sign of the MR with the existence of the scaling law, or with the value of the coefficient α , or with the temperature profile of the conductance. Consequently, the origin

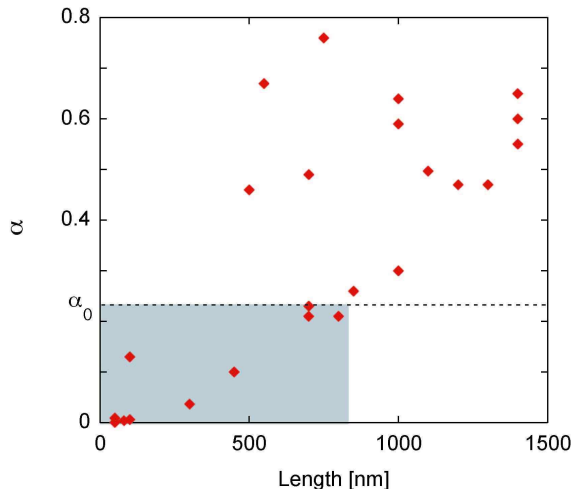


FIG. 3: Scaling coefficient α as a function of the length of the MWNT. The grey zone corresponds to $\alpha \leq \alpha_0$, where α_0 is the theoretical value calculated for a Luttinger liquid.

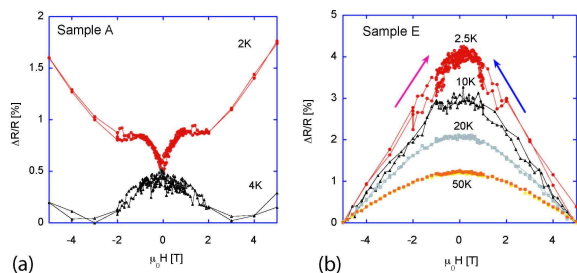


FIG. 4: Magnetoresistance profile at large fields for samples A (the curve is shifted by 0.5% for clarity) and E. Sample A has a negative MR at low temperature and sample E has a positive MR.

of this behavior must be ascribed to a small numbers of dopants, which modify strongly the Fermi level from one sample to the other [22], but do not modify significantly α .

At low magnetic field, the magnetization of the wire (bottom electrode) is oriented at an angle of 90° with respect to the Ni layer (top electrode). The magnetization of the Ni wire rotates uniformly with increasing the

applied field (following the Stoner-Wohlfarth curve [23]), reaching the parallel configuration at about 0.6 to 1.5 Tesla, depending on the length of the Ni wire. The measurements as a function of weak external fields give then access to the conductance as a function of the angle of the two ferromagnetic contacts (the so called SD-MR, i.e. the effect of the spin polarization of the current). Note that the antiparallel configuration is not reached in these measurements. The efficiency of spin-injection process in a Ni nanowire (without carbon nanotube) has been observed by a current-induced magnetization-reversal effect in previous experiments [23]. With respect to the SD-MR, the surprising result of the present study is that the MR measured at reasonable current values (injected current of about $1 \mu\text{A}$) is always very small, below 1 % of the total resistance, whatever the length of the tube from 150 nm to 1500 nm (see also Ref. [4]). Three different kinds of SD-MR are observed, which are illustrated in Fig. 5 with samples **A** to **D**. In sample **B** (Fig. 5(b)), for small tubes the well-known AMR of the Ni wire is measured where AMR signal is easily identified by the typical shape as a function of the angle of the applied field [23]. The AMR is about 1.8Ω , i.e. 0.13 % of the total resistance, and $\alpha=0.037$. The AMR signal shows that the current is spin polarized and that the tube does not play any role in the MR. In sample **C** (Fig.5(c)), a second type of SD-MR hysteretic response is also measured with $\Delta R = 20 \Omega$ (about 0.7 % of the total resistance). In such cases, an important ZBA is observed, but the conductivity cannot be scaled with power law. The SD-MR is observed at low temperature only, and disappears between 4K and 8K. This behavior as a function of magnetic field and temperature is typical for a very bad tunneling junction [23]. In sample **A** (presented in Fig. 2) and sample **D** (for which $\alpha = 0.59$), a third type of SD-MR can be measured *which depends on the direction of the current*. Such SD-MR is dramatically enhanced at very small or zero bias (see Ref. [3]) because it is due to the electrochemical potential difference between the ferromagnet and the quantum wire. This SD-MR disappears at temperatures above 8K. This behavior can be understood within the hypothesis of a non-equilibrium spin-injection that depends on the incident spin-polarization of the current. The spin-injection from the ferromagnet, where the electrons are spin polarized, to the quantum wire is not equivalent to the spin-injection from the quantum wire (where there is no spin polarization of the current) to the ferromagnet. These observations may corroborate some predictions about non-equilibrium transport effects due to spin-charge separation [10].

In conclusion, we have measured the spin-dependent transport properties of a series of MWNTs of various lengths, contacted by ferromagnetic Ni electrodes. Most of the samples exhibit a typical scaling law behavior of the zero bias anomaly as a function of the temperature. We observed furthermore that the magnetoresistance due to the spin polarization of the current is systematically destroyed in the nanotube. Only the AMR of the elec-

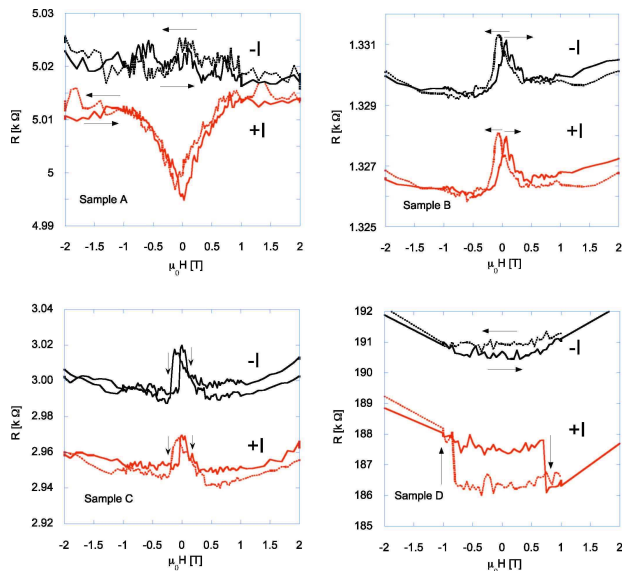


FIG. 5: Spin-dependent magnetoresistance for four samples. (a) Sample A, (b) Sample B : AMR response $\alpha = 0.037$; (c) sample C : ZBA and no scaling property; (D) Sample D, $\alpha = 0.6$.

trodes and some weak interface or reservoir effects (spin-injection) are observed. If we assume that the observed scaling is due to the manifestation of strong electron-electron interactions with scattering between different modes, the destruction of spin-dependent magnetoresistance leads then to a spin-diffusion lengths below 150 nm. This is in contradiction with the semi-ballistic properties of nanotubes. Consequently, these results can be interpreted assuming that the scaling law $GT^{-\alpha}(eV_{bias}/kT)$ originates from Luttinger Liquid behaviour, and that the suppression of the spin dependent magnetoresistance is due to spin-charge separation.

Acknowledgments

This work was supported by the grant n° 21-61550 of the Swiss National Science Foundation. We are grateful to the Centre Interdépartmental de Microscopie Electronique of EPFL (CIME-EPFL) for access to electron microscopy facilities. We acknowledge enlightening discussions with R. Egger, S. Roche, A. Bachtold and C. Schoenenberger about spin dependent magnetoresistance in carbon nanotubes.

-
- [1] G.A. Prinz, *Science* **282**, 1660 (1998).
 - [2] K. Tsukagoshi, B. W. Alphenaar, and H. Ago, *Nature (London)*, **401** and 572 (1999) and B. W. Alphenaar, K. Tsukagoshi, M. Wagner, *J. Appl. Phys.* **89**, 6863 (2001).
 - [3] B. Zhao, I. Moench, H. Vinzelberg, T. Muehl, and M. Schneider, *Appl. Phys. Lett.* **80**, 3144 (2002) and B. Zhao, I. Moench, H. Vinzelberg, T. Muehl, and M. Schneider, *J. Appl. Phys.* **91** 7026 (2002).
 - [4] D. Orgassa, G. J. Mankey, H. Fujiwara, *Nanotechnology* **12**, 281 (2001).
 - [5] J. Haruyama, I. Takesue and Y. Sato, *Appl. Phys. Lett.* **77**, 2891 (2000) and *Phys. Rev. B.* **63**, 073406 (2001), J. Haruyama, I. Takesue, Syu Kato, Kazuya Takazawa, and Yuki Sato, *Appl. Surf. Science* **175**, 597 (1995).
 - [6] J. Voit, *Rep. Prog. Phys.* **58**, 977 (1995).
 - [7] T. Lorenz, M. Hofmann, M. Grueninger, A. Freimuth, G. S. Uhrig, M. Dumm and M. Dressel, *Nature (London)* **418**, 614 (2002).
 - [8] C. L. Kane, M. P. A. Fisher, *Phys. Rev. B* **46**, 15233 (1992).
 - [9] Q. Si, *Phys. Rev. Lett.* **81**, 3191 (1998).
 - [10] L. Balents, R. Egger, *Phys. Rev. Lett.* **85**, 3464 (2000) and *Phys. Rev. B* **64**, 035310 (2001).
 - [11] H. Mehrez, J. Taylor, H. Guo, J. Wang, and C. Roland, *Phys. Rev. Lett.* **84**, 2682 (2000).
 - [12] C. Schoenenberger, A. Bachtold, C. Strunk, J.-P. Salvetat, L. Forro, *Appl. Phys. A* **69** 283 (1999).
 - [13] M. Bockrath, D. H. Cobden, J. Lu, A. G. Rinzler, R. E. Smalley, L. Balents, and P. L. McEuen, *Nature (London)*, **397**, 598 (1999).
 - [14] Z. Yao, H. W. C. Postma, L. Balents, and C. Dekker, *Nature (London)* **402**, 273 (1999).
 - [15] H. W. C. Postma, M. de-Jonge, and C. Dekker, *Phys. Rev. B*, **62**, R10653 (2000).
 - [16] A. Bachtold, M. de Jonge, K. Grove Rasmussen, and P. L. McEuen, *Phys. Rev. Lett* **87**, 166801 (2001).
 - [17] C. L. Kane, L. Balents, and M.P.A. Fisher, *Phys. Rev. Lett.* **79**, 5086 (1997).
 - [18] R. Egger, *Phys. Rev. Lett.* **83**, 5547 (1999).
 - [19] R. Egger, A. O. Gogolin, *Chem. Phys.* **281**, 447 (2002).
 - [20] M. W. Bockrath, *Carbon Nanotubes Electrons in One dimension*, Ph.D. thesis, University of California, Berkeley, 1999.
 - [21] R. Tarkiainen, M. Ahlskog, J. Penttila, L. Roschier, P. Hakonen, M. Paalanen, and E. Sonin, *Phys. Rev. B*, **64**, 195412 (2001).
 - [22] S. Roche and R. Saito, *Phys. Rev. Lett.* **87** (2001), 246803.
 - [23] J-E Wegrowe, D. Kelly, A. Franck, S. Gilbert, J.-Ph. Ansermet *Phys. Rev. Lett.* **82** (1999), 3681, J-E. Wegrowe et al. *Phys. Rev B*, **61**, 12216 (2000) and *Phys. Rev B* **65**, 012407 (2001) and *J. Appl. Phys.* **91**, 6806 (2001).